Experimental Investigation of Phase Coded FMCW for Sensing and Communications

Kumbul, Utku; Petrov, Nikita; van der Zwan, Fred; Vaucher, Cicero S.; Yarovoy, Alexander

DOI
10.23919/EuCAP51087.2021.9411464

Publication date
2021

Document Version
Final published version

Published in
2021 15th European Conference on Antennas and Propagation (EuCAP)

Experimental Investigation of Phase Coded FMCW for Sensing and Communications

Utku Kumbul*, Nikita Petrov*, Fred van der Zwan*, Cicero S. Vaucher†* and Alexander Yarovoy*
* Department of Microelectronics, Delft University of Technology, Delft, The Netherlands
† NXP Semiconductors, Eindhoven, The Netherlands
{u.kumbul, n.petrov, w.f.vanderzwan c.silveiravaucher, a.yarovoy}@tudelft.nl

***Abstract*—The phase coded FMCW and its properties for joint sensing and communication are studied. Two different receiver structures for the sensing properties of this waveform are compared theoretically and experimentally. It is shown both by simulations and experiments that the phased coded FMCW combines communication capabilities of PMCW and sensing capabilities of FMCW while using a realizable hardware complexity for an automotive radar.**

***Index Terms*—Phase coding, FMCW, PMCW, joint sensing and communication, phase coded FMCW.**

I. Introduction

The joint sensing and communication systems have gathered a growing interest in autonomous driving as the radio frequency spectrum is densely occupied [1], [2]. The conventional autonomous driving systems use radar sensors for sensing and separate communication wireless systems to provide vehicle-to-vehicle (V2V) communication. Both of these two functionalities use the available spectrum and hence operating multiple autonomous driving vehicles on the road causes spectral congestion [3]. To cope with this problem, various waveform designs are investigated to combine sensing and communication functions [4]–[7]. One of the cost efficient solutions is to use available radar waveform on autonomous driving systems and modulate it with the communication signal to provide joint sensing and communication.

The frequency modulated continuous waveform (FMCW) has been commonly used in automotive radar applications due to its low sampling requirements and simple hardware design. The FMCW automotive radar uses dechirping receiver where the received signal is mixed with the transmitted signal to obtain the beat signal. Subsequently, range and velocity information of the targets are extracted from the beat signal using two-dimensional Fourier transform [8]. Despite providing good sensing performance, FMCW radar is weak against radar to radar interference and its detection performance is degraded in presence of interference [9].

The phase modulated continuous waveform (PMCW) owns high robustness of the radar against interference [10]. Moreover, the PMCW has ability to carry information and has been mostly used for communication purposes [11]. In PMCW, the phase of the transmitted waveform is changed according the code sequence. The received signal is downconverted to the baseband and match filter is applied. However, the PMCW is sensitive to the Doppler frequency shift (no Doppler tolerant) and requires high sampling frequency of the receiver. These limitations of PMCW prevent its wide usage in automotive radars [11].

Lately, the phase coded frequency modulated continuous waveform (PC-FMCW) has received remarkable attention due to combining the advantages of both FMCW and PMCW [12]. Applying phase coding to FMCW provides unique features such as enabling joint radar-communication (RadCom) coexistence [13] and improving resilience to mutual interference [14]. However, the experimental investigation about the impact of coding on sensing and communication has not been studied.

In this paper, we investigate phase coded FMCW and demonstrate its applicability for both sensing and communication. We analyze and compare two different receiver structures for the sensing capability of PC-FMCW. The simulation and experimental results show that the PC-FMCW radar can ensure similar sensing performance of uncoded FMCW for a short-range radar while providing V2V communication with a realizable hardware complexity for an automotive sensor.

The rest of the paper is organised as follows. Section II provides the signal model while Section III explains the waveform properties. Section IV illustrates the experimental results and Section V presents conclusion remarks.

II. Signal Model

The linear frequency modulated continues waveform (LFMCW) can be written as

$$x_{\mathrm{LFM}}(t) = \cos\left(2\pi f_c t + \pi\frac{B}{T}t^2\right),\ t \in [0,\, T] \tag{1}$$

where f_c is the carrier frequency, B is the bandwidth and T is the sweep duration of the signal. In PC-FMCW case, a code sequence is used to modulate the phase of the signal [12] such that

$$x_{\mathrm{T}}(t) = \cos\left(2\pi f_c t + \pi\frac{B}{T}t^2 + \phi(t)\right), \tag{2}$$

where $\phi(t)$ is the instantaneous phase. We chose binary phase shift keying (BPSK) as code modulation scheme where phase changes between $\{0, \pi\}$, then the transmitted PC-FMCW signal can be represented as

$$x_{\mathrm{T}}(t) = \sum_{n=1}^{L_c} e^{j\phi_n} \mathrm{rect}\left(\frac{t-(n-1/2)T_c}{T_c}\right) \times \cos\left(2\pi f_c t + \pi \frac{B}{T} t^2\right), \tag{3}$$

where L_c is the code length, $T_c = T/L_c$ is the chip duration and rect is the rectangle function. The received signal reflected from target can be obtained as

$$x_{\mathrm{R}}(t) = \sum_{n=1}^{L_c} e^{j\phi_n} \mathrm{rect}\left(\frac{t-\tau-(n-1/2)T_c}{T_c}\right) \times \cos\left(2\pi f_c (t-\tau) + \pi \frac{B}{T} (t-\tau)^2\right), \tag{4}$$

where τ is the round trip delay between radar and target. In the following subsections, we will investigate two different receiver structures for sensing performance of PC-FMCW.

A. Matched filtering

In the matched filtering, the received signal is convoluted with the complex conjugate of the transmitted signal to maximize the signal to noise ratio (SNR) as

$$x_{\mathrm{m}}(t) = \int_{-\infty}^{\infty} x_{\mathrm{R}}(m)\, x_{\mathrm{T}}{}^{*}(t-m)\, dm, \tag{5}$$

where $*$ denotes the complex conjugate. The range and velocity information of the targets can be extracted from the output of the matched filter.

B. Dechirping and decoding

In decirping and decoding receiver structure, the received signal is mixed with uncoded LFMCW signal for dechirping (downconversion) process and low pass filtered (LPF) to eliminate high frequency terms [14]. The filtered mixer output gives the coded beat signal as

$$b_{\mathrm{c}}(t) = \sum_{n=1}^{L_c} e^{j\phi_n} \mathrm{rect}\left(\frac{t-\tau-(n-1/2)T_c}{T_c}\right) \times \cos\left(2\pi f_c \tau + 2\pi \frac{B}{T} \tau t - \pi \frac{B}{T} \tau^2\right). \tag{6}$$

In the decoding process, the coded beat signal is multiplied with the complex conjugate of the code to correct the phase changes initiated by the phase code. It is not possible to apply one decoding signal since each coded beat signal has different time delay due to being reflected from a target at a particular range. However, this can be corrected by aligning the received beat signals either in frequency [13] or time domain [14] processing. Finally, the decoded beat signal can be written as

$$b(t) = \cos\left(2\pi f_c \tau + 2\pi \frac{B}{T} \tau t - \pi \frac{B}{T} \tau^2\right). \tag{7}$$

Here, the second term is known as the beat frequency $f_b = \tau B/T$ in which range and velocity information of the target embedded. This target information can be extracted by applying spectral estimation techniques in traditional range-Doppler processing.

TABLE I
SYSTEM PARAMETERS

Bandwidth	B	$40MHz$
Chirp duration	T	$1ms$
Sampling frequency	f_s	$400MHz$
Intermediate frequency	f_{IF}	$125MHz$
Carrier frequency	f_c	$3.315GHz$
Number of pulse	N_p	128
Code length	L_c	1024
Chip duration	T_c	$0.97\mu s$
Chip bandwidth	B_c	$1.024MHz$

III. Waveform Properties

A. Sensing Performance

In this section, we evaluate the sensing performance of the PC-FMCW by investigating its ambiguity function. The ambiguity function corresponds to the outcome of matched filter and it determines range-Doppler resolution of the transmitted signal. The ambiguity function of PC-FMCW can be calculated as

$$|\,\chi(\tau; f_d)\,| = \left| \int_{-\infty}^{\infty} x_{\mathrm{T}}(t)\, x_{\mathrm{T}}{}^{*}(t-\tau) e^{j2\pi f_d t}\, dt \right|, \tag{8}$$

where f_d represents the Doppler frequency. The ambiguity function of the PC-FMCW with parameters given in Table I is presented in Figure 1. As we are interested in automotive radar application, we select parameters appropriate for such application but scaled them down to S-band. Note that the 1 kHz Doppler frequency corresponds to a target with radial velocity 1.9 m/s at 79 GHz and 45 m/s at 3.3 GHz.

For sensing property of PC-FMCW, different range profiles can be obtained depending on the code length and code family [15], [16]. In this paper, we used zero-correlation zone (ZCZ) codes and we simulate the range cuts of the ambiguity function with various code lengths. As seen in Figure 2, the sidelobes level is raising as the code length increases. The impact of the code length on the sidelobes is investigated with the integrated sidelobe level (ISL) [16]

$$ISL = \int_{-\infty}^{\infty} |\,\chi(\tau \neq 0; f_d = 0)\,|\, d\tau. \tag{9}$$

In Figure 3, the ISL is shown as the function of the code lengths and the ISL increases up to -47 dB for $L_c = 1024$. However, sidelobes level is similar to FMCW for short range radar applications where the maximum range is 100 m.

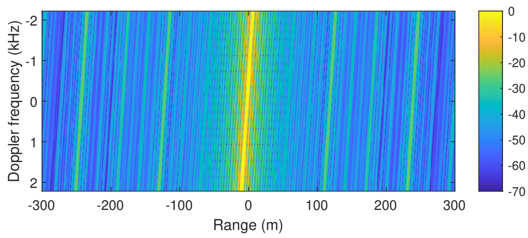

Fig. 1. Ambiguity function of the phase coded frequency modulated waveform for $L_c = 1024$.

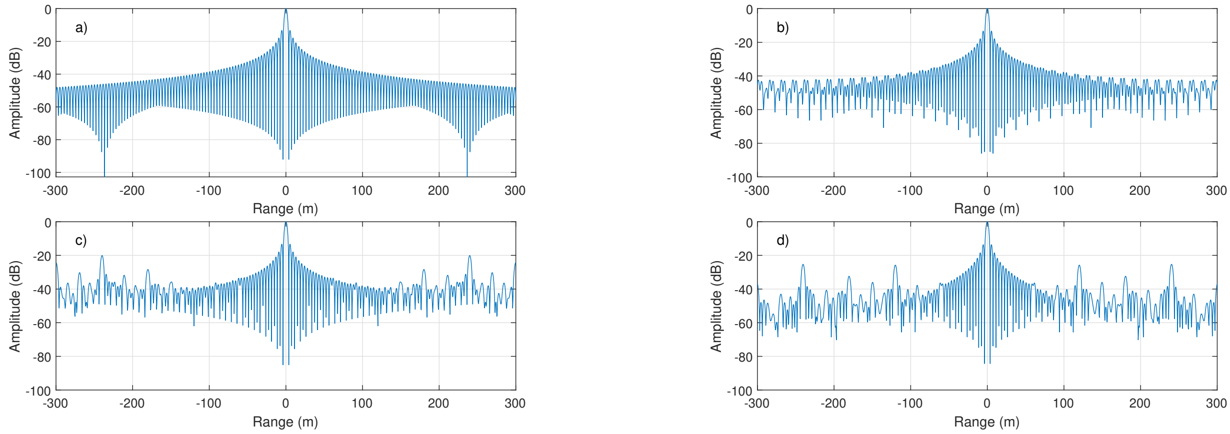

Fig. 2. Range cuts of the ambiguity function with different code length; a) LFMCW, b) $L_c = 4$, c) $L_c = 64$, d) $L_c = 1024$

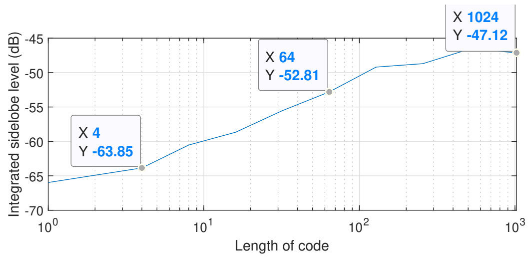

Fig. 3. Integrated sidelobe level vs the code lengths

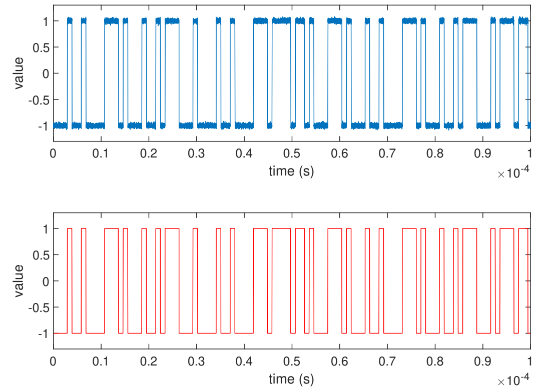

Fig. 5. Received communication signal; after band-pass filter (blue), after threshold (red)

B. Communication

Below, we illustrate the communication capability of PC-FMCW. To extract the communication signal, the delay between transmitted and received signal needs to be compensated. In [7], synchronized LFMCW signal is generated to minimize the delay by using GPS. Similarly, we assume the synchronized LFMCW is obtained in the receiver and used for dechirping as shown in Figure 4. The synchronized LFMCW can be written as

$$\bar{x}_{\mathrm{T}}(t) = \cos\left(2\pi f_c(t-\tau) + \pi\frac{B}{T}(t-\tau)^2\right). \qquad (10)$$

The received signal is mixed with synchronized LFMCW signal and filtered to get rid of the chirp signal. At the outcome of mixer, the beat frequency signal will have either zero carrier frequency for stationary transmitter and receiver or small (in comparison to the modulated frequency) frequency offset for mutually moving transmitter and receiver. After LPF, the received communication signal with delay is obtained as

$$\begin{aligned} x_{\mathrm{c}}(t) &= [x_{\mathrm{R}}(t) + n(t)]\; \bar{x}_{\mathrm{T}}(t) \\ &= \sum_{n=1}^{L_c} e^{j\phi_n} \mathrm{rect}\left(\frac{t-\tau-(n-1/2)T_c}{T_c}\right) + \bar{n}(t) \qquad (11) \\ &= c(t-\tau) + \bar{n}(t), \end{aligned}$$

where $n(t)$ and $\bar{n}(t)$ represent the additive white Gaussian noise and $c(t-\tau)$ denotes the delayed communication signal. After delay compensation, we apply base-band filter and threshold to reconstruct the transmitted communication signal which carries up to 1 Mbit/s information, as shown in Figure 5.

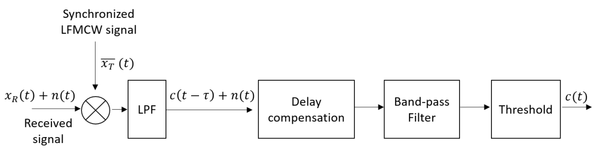

Fig. 4. Block diagram of communication

IV. Experiment Results

The experimental study of PC-FMCW has been done using PARSAX radar [17]. We use ZCZ codes and select the system parameters as shown in Table I to detect both stationary and moving targets.

A. Stationary Target Experiment

We start with observing the chimney as stationary target which is 1185 m away from the radar. For dechirping and

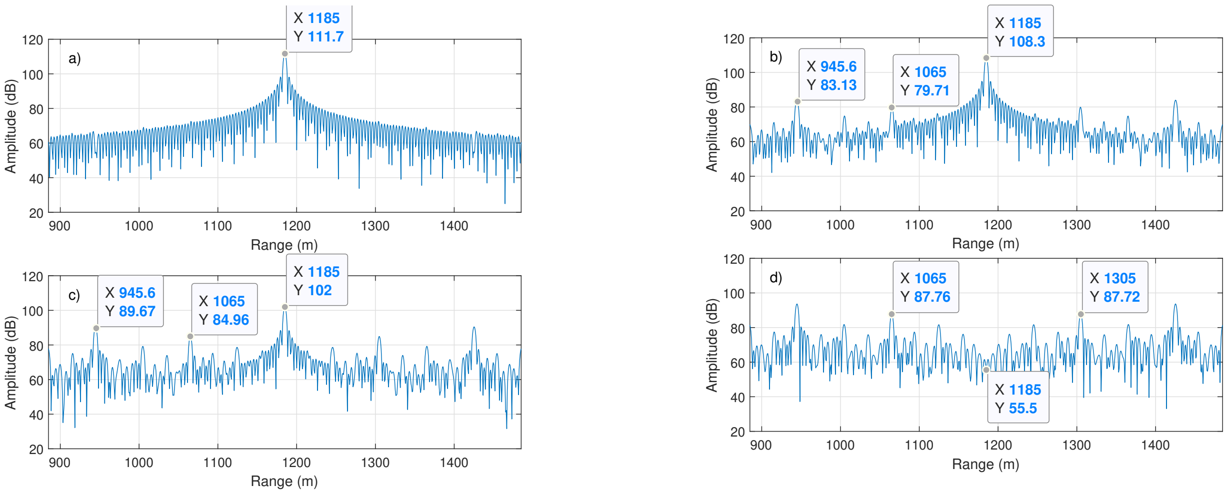

Fig. 6. Decoding simulation with the reference code away from the target; a) $R = 5$ m , b) $R = 50$ m, c) $R = 100$ m, d) $R = 150$ m

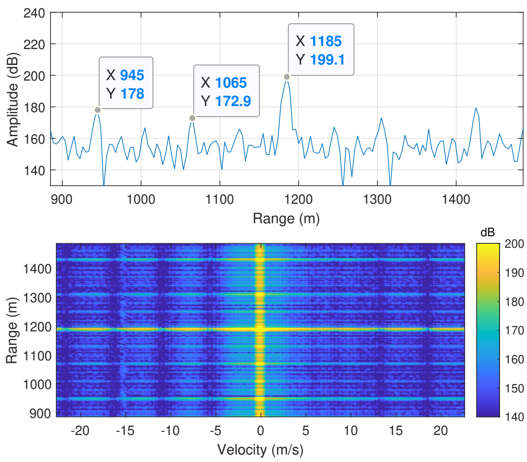

Fig. 7. Dechirping and decoding with reference delay $R = 50$ m for stationary target; range and range-Doppler map

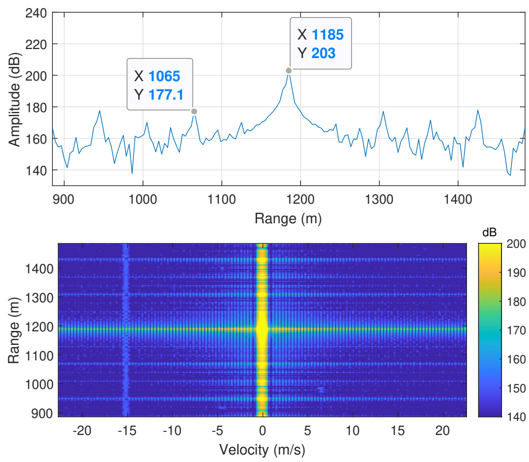

Fig. 8. Matched filter response for stationary target; range and range-Doppler map

decoding receiver structure, each coded beat signal has different time delay and thus they need to be aligned for ideal decoding. However, the time delay can be negligible if the target is very close to the radar. To mimic short range radar scenario with this experimental setup, we can use the reference transmitted signal which is close to the target. As seen in Figure 6, range profiles after decoding are still tolerable with a target up to $R = 100$ m away from the reference transmitted signal while the target location is completely lost when a target is at $R = 150$ m away. This relation can also be observed with the sidelobes of coding signal shown in Figure 2 d. In the following experimental results for dechirping and decoding receiver structure, we consider short range radar application and use the reference transmitted signal for decoding at $R = 50$ m away from the target. As shown in Figure 7, the peak location of the target is obtained at 1185 m when we decode with reference delay. Note that we have $10\log_{10}(\mathrm{N})$ processing gain where N is the number of pulses used for Doppler processing. For the second receiver structure, the received signal is processed by the matched filtering. The range profile acquired by the matched filter process is similar to its ambiguity function and the peak location of the target is obtained at 1185 m as demonstrated in Figure 8. Note that the dynamic ranges of both receivers (ratio between peak to first sidelobe ratio) are similar.

B. Moving Target Experiment

At the next stage, we observe a moving car with a radial velocity 15 m/s and located 1178 m away from the radar. For dechirping and decoding receiver structure with reference delay, the peak location of the moving target is observed at 1178 m as illustrated in Figure 9. Finally, we apply the matched filter to obtain the range-Doppler map of the moving target. As seen in Figure 10, we obtain the peak location of the moving target at 1178 m. Likewise to stationary target case, the dynamic ranges of both receivers are similar.

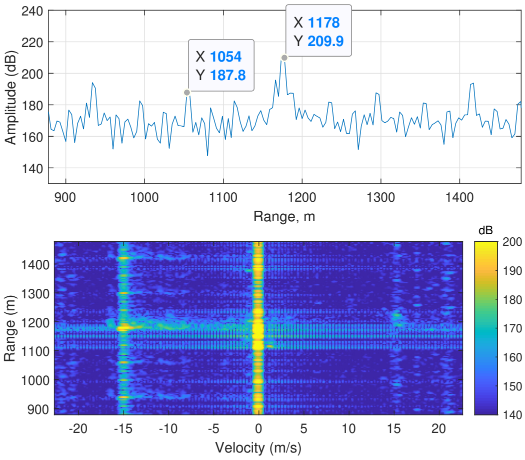

Fig. 9. Dechirping and decoding with reference delay $R = 50$ m for moving target; range and range-Doppler map

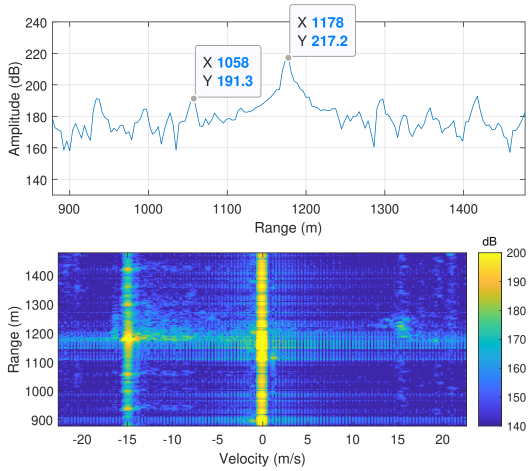

Fig. 10. Matched filter response for moving target; range and range-Doppler map

V. Conclusion

The properties of the phased coded FMCW for sensing and communication purposes have been studied analytically and verified experimentally. We have demonstrated that the integrated sidelobe level of the ambiguity function grows with the increase of data rate. For a short-range radar application with the maximal range of 100 m, the investigated waveform provides a communication data rate up to 1 Mbit/s and sensing capabilities comparable to LFMCW. The hardware and software complexity, in particular the ADC sampling rate, remains at a realizable level for an automotive radar. The higher communication capabilities can be achieved with the price of higher range sidelobes or with the increase of ADC sampling rate.

Acknowledgment

This project is funded through the TU Delft Industry Partnership Programme (TIPP) from NXP Semiconductors N.V. and Holland High Tech Systems and Materials (TKI-HTSM/18.0136) under the project "Coded-radar for Interference Suppression in Super-Dense Environments" (CRUISE).

The authors would like to thank Oleg Krasnov for his support during the experiments.

References

[1] K. V. Mishra, M. R. Bhavani Shankar, V. Koivunen, B. Ottersten, and S. A. Vorobyov, "Toward millimeter-wave joint radar communications: A signal processing perspective," *IEEE Signal Processing Magazine*, vol. 36, no. 5, pp. 100–114, 2019.

[2] F. Liu, C. Masouros, A. Petropulu, H. Griffiths, and L. Hanzo, "Joint radar and communication design: Applications, state-of-the-art, and the road ahead," *IEEE Transactions on Communications*, vol. 68, pp. 3834–3862, 2020.

[3] C. Aydogdu, M. F. Keskin, G. K. Carvajal, O. Eriksson, H. Hellsten, H. Herbertsson, E. Nilsson, M. Rydstrom, K. Vanas, and H. Wymeersch, "Radar interference mitigation for automated driving: Exploring proactive strategies," *IEEE Signal Processing Magazine*, vol. 37, no. 4, pp. 72–84, 2020.

[4] R. M. Gutierrez, H. Yu, A. R. Chiriyath, G. Gubash, A. Herschfelt, and D. W. Bliss, "Joint sensing and communications multiple-access system design and experimental characterization," in *2019 IEEE Aerospace Conference*, 2019, pp. 1–8.

[5] C. Aydogdu, M. F. Keskin, N. Garcia, H. Wymeersch, and D. W. Bliss, "RadChat: Spectrum sharing for automotive radar interference mitigation," *IEEE Transactions on Intelligent Transportation Systems*, vol. 22, no. 1, pp. 416–429, 2021.

[6] P. M. McCormick, C. Sahin, S. D. Blunt, and J. G. Metcalf, "FMCW implementation of phase-attached radar-communications (PARC)," in *2019 IEEE Radar Conference (RadarConf)*, 2019, pp. 1–6.

[7] F. Lampel, F. Uysal, F. Tigrek, S. Orru, A. Alvarado, F. Willems, and A. Yarovoy, "System level synchronization of phase-coded FMCW automotive radars for RadCom," in *2020 14th European Conference on Antennas and Propagation (EuCAP)*, 2020, pp. 1–5.

[8] M. Jankiraman, *FMCW Radar Design*. Massachusetts: Artech House, 2018.

[9] F. Roos, J. Bechter, C. Knill, B. Schweizer, and C. Waldschmidt, "Radar sensors for autonomous driving: Modulation schemes and interference mitigation," *IEEE Microwave Magazine*, vol. 20, no. 9, pp. 58–72, 2019.

[10] V. Giannini, D. Guermandi, Q. Shi, A. Medra, W. Van Thillo, A. Bourdoux, and P. Wambacq, "A 79 GHz phase-modulated 4 GHz-BW CW radar transmitter in 28 nm CMOS," *IEEE Journal of Solid-State Circuits*, vol. 49, no. 12, pp. 2925–2937, 2014.

[11] S. Alland, W. Stark, M. Ali, and M. Hegde, "Interference in automotive radar systems: Characteristics, mitigation techniques, and current and future research," *IEEE Signal Processing Magazine*, vol. 36, no. 5, pp. 45–59, 2019.

[12] J. Reneau and R. R. Adhami, "Phase-coded LFMCW waveform analysis for short range measurement applications," in *2014 IEEE Aerospace Conference*, 2014, pp. 1–6.

[13] F. Lampel, R. F. Tigrek, A. Alvarado, and F. M. J. Willems, "A performance enhancement technique for a joint FMCW RadCom system," in *2019 16th European Radar Conference (EuRAD)*, 2019, pp. 169–172.

[14] F. Uysal, "Phase-coded fmcw automotive radar: System design and interference mitigation," *IEEE Transactions on Vehicular Technology*, vol. 69, no. 1, pp. 270–281, 2020.

[15] E. García, J. A. Paredes, F. J. Álvarez, M. C. Pérez, and J. J. García, "Spreading sequences in active sensing: A review," *Signal Processing*, vol. 106, pp. 88 – 105, 2015.

[16] A. Alejos, M. Dawood, and H. Mohammed, "Estimation of sidelobe level variations of phased codes in presence of random interference for bistatic wideband noise radar," *International Journal of Antennas and Propagation*, vol. 2015, pp. 1–11, 04 2015.

[17] O. A. Krasnov, L. P. Ligthart, Zhijian Li, P. Lys, and F. van der Zwan, "The PARSAX - full polarimetric FMCW radar with dual-orthogonal signals," in *2008 European Radar Conference*, 2008, pp. 84–87.